Eur. Phys. J. C 9, 181–195 (1999)
DOI 10.1007/s100529900050

THE EUROPEAN PHYSICAL JOURNAL C

Restoring good high energy behaviour in Higgs production via W fusion at the LHC

K. Philippides[1], W.J. Stirling[1,2]

[1] Department of Physics, University of Durham, Durham, DH1 3LE, UK
[2] Department of Mathematical Sciences, University of Durham, Durham, DH1 3LE, UK

Received: 30 January 1999 / Published online: 20 May 1999

Abstract. The W-fusion scattering process $W^+W^- \to ZZ$ for off-shell W bosons is studied, focusing on the issue of its high-energy behaviour which is known to be anomalous. It is shown that the unitarity violating terms can be isolated and extracted in a well-defined and efficient way using the pinch- technique. This restores the good high energy behaviour of the cross section and, in particular, makes possible the identification of the Higgs resonance in the invariant mass distribution m_{ZZ} of the Z pair. The discarded terms, which are proportional to the off-shellness of the W bosons, cancel against similar terms originating from the remaining diagrams for the full physical process $f_1 f_2 \to \overline{f'}_1 \overline{f'}_2 ZZ$. This cancellation ensures the gauge invariance of our result, which therefore constitutes a meaningful separation between *signal* and *background* when they both contribute coherently. Equipped with this result, we are able to define a resonant approximation for the process $pp \to ZZ + 2$ jets $+ X$, which circumvents the problem of good high energy behaviour without having to resort to the lengthy calculation of the complete set of diagrams. In this approximation only the W- and Z-fusion *signal* graphs are included, i.e. the ones which contain the Higgs resonance. We have verified that the approximate resonant cross section describes very well the full result not only close to the resonance but also beyond it.

1 Introduction

The discovery of the Higgs boson is the primary physics goal of the LHC pp collider. For low Higgs masses the dominant production mechanism is gluon fusion, $gg \to H$, but for a heavy Higgs there is also a significant contribution from the W-fusion process, $WW \to H$, where the Ws are emitted from incoming quarks.[1] Since a heavy (Standard Model) Higgs is most easily detected in the ZZ decay channel, the process of interest is $WW \to H \to ZZ$. However the s-channel Higgs resonant diagram is only one of several diagrams contributing to this scattering process, the other diagrams containing, for example, trilinear and quadrilinear gauge boson vertices. In fact the W-fusion process

$$W(p_1)W(p_2) \to Z(k_1)Z(k_2) \tag{1.1}$$

provides a classic illustration of the subtle gauge cancellations encountered in non-Abelian gauge theories. The role of the Higgs graph is crucial in obtaining a cross section which is well behaved at high energies, see for example the discussion in [1]. In practice, however, one actually has to consider the case of *off-shell* W-fusion, since Ws emitted from the incoming quarks have $q^2 < 0$. But when the Ws are *off-shell* the delicate gauge cancellations responsible for the good high energy behaviour of the amplitude are spoiled. Unitarity is badly violated by terms which are proportional to the *off-shellness* of the Ws [2],

$$W_1 = p_1^2 - M_W^2$$
$$W_2 = p_2^2 - M_W^2 \ . \tag{1.2}$$

Unitarity is only restored for the physical cross section when the *full* set of diagrams for the $qq \to qqZZ$ process is taken into account [2], [3], i.e. not just the subset containing $WW \to ZZ$. This involves a very large number of additional Feynman graphs.

Since in the region of $M_{ZZ} \sim M_H$ the *on-shell* $WW \to ZZ$ proces is clearly well approximated by the s-channel Higgs resonance graph (at least for M_H not too large so that $\Gamma_H \ll M_H$), it is interesting to ask whether the full $qq \to qqZZ$ process, including off-shell WW scattering, can be similarly approximated, while retaining good high-energy behaviour. In other words, one seeks a minimal set of diagrams that include the Higgs resonance while at the same time not spoiling the delicate gauge cancellations.

To begin with one could consider only the Higgs resonant diagram contributing to $qq \to qqZZ$. However this leads to a cross section that behaves badly at high energies, growing like s. As a result the shape of the differential cross section around the resonance cannot be trusted. As a next step one could extend the set to contain all six of the W-fusion diagrams of process (1.1). As already mentioned, there *are* potential cancellations at high energy in this case but the cross section actually respects unitarity only when both Ws are *on-shell*. In the *off-shell* case when

[1] See, for example, the review in [1].

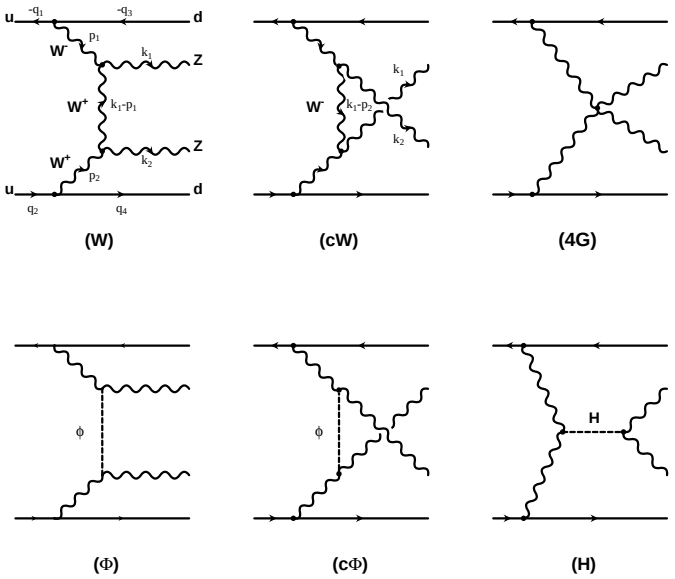

Fig. 1. The six W fusion graphs T_{WW} and relevant kinematics

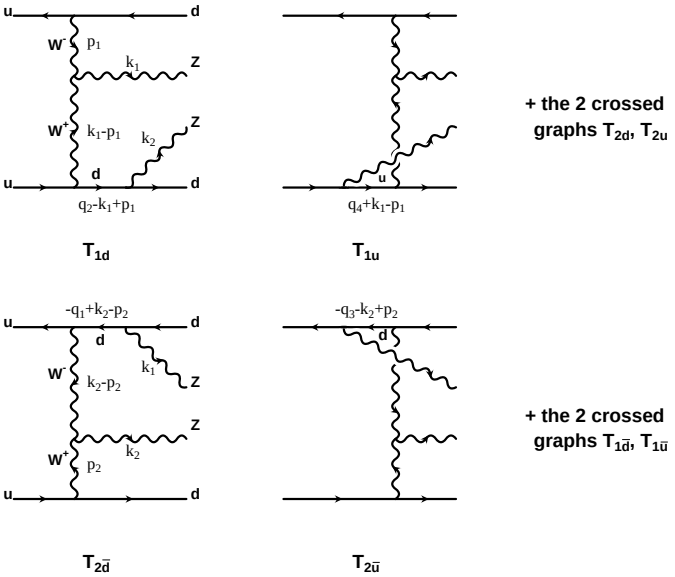

Fig. 2. The T_{Wf} graphs. The relevant kinematics are also shown. Crossed graphs are omitted

the six diagrams are embedded in $qq \to qqZZ$, see Fig. 1, this is not true anymore and in fact the situation gets even worse. The cross section now grows as s^2 with the leading terms always proportional to the *off-shellness* of the Ws, i.e. W_1 and W_2. For high enough energies the Higgs resonance gets completely swamped by these *off-shell* terms and the differential cross section exhibits no resonance structure. Only when the full set of graphs (Figs. 1–3) is considered does one obtain a cross section that behaves well at high energies. In this set large gauge cancellations take place and the resulting cross section exhibits the same behaviour as for *on-shell* Higgs production through the process $qq \to qqH$, namely it grows slowly as $\ell n(s)$ for large s.

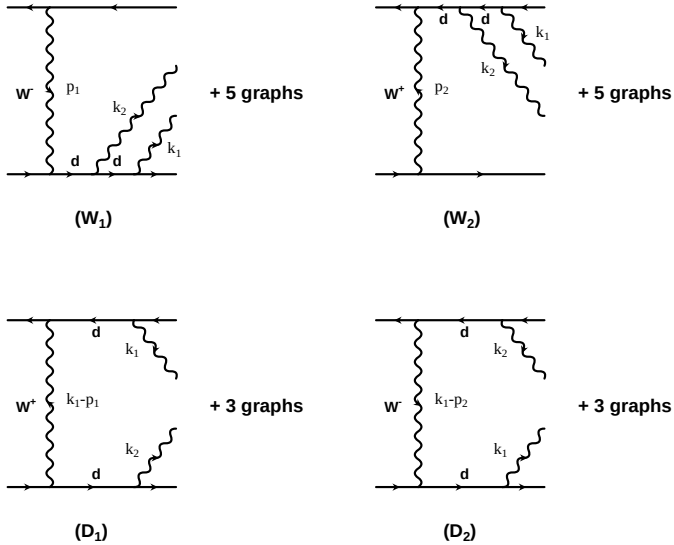

Fig. 3. The T_{ff} graphs. The graphs not shown refer to permutations of the relative positions of the Z bosons on the fermion line to which they are attached

The bad high-energy behaviour of individual diagrams can be attributed to the following two factors: i) the presence of the trilinear gauge boson vertices, and ii) the fact that the Z bosons can be longitudinally polarized. Both these factors bring extra momenta in the numerator of Feynman graphs. In fact the polarization vector of an energetic longitudinal Z boson behaves as

$$\epsilon_L^\mu(k_1) = \frac{k_1^\mu}{M_Z} + \mathcal{O}(M_Z/E_Z) \ . \tag{1.3}$$

As a result of the M_Z factor in the denominator, the cross section can grow as powers of s/M_Z^2. However the momenta introduced by these factors into the numerator of the Feynman graphs are at the same time the momenta which make possible a 'communication' between graphs with seemingly different propagator structures. It is this communication that eventually leads to the gauge cancellations between different diagrams that restore the good high-energy behaviour. Obviously the cancellation of gauge-dependent terms between different graphs will be even more pronounced in a general R_ξ gauge, due to the presence of the extra momenta in the longitudinal part of a gauge boson's propagator in this case.

Any attempt to approximate Higgs production using only resonant production via WW fusion (or indeed any other multi-gauge-boson production process) cannot therefore succeed unless the above gauge cancellations are correctly taken into account. The recently developed *tree level pinch technique* [4], [5], provides exactly the right calculational framework for addressing this problem. It allows a rigorous definition of a gauge invariant subamplitude which can be used to approximate a full scattering amplitude. For example in [4], the authors considered the process $e^+e^- \to W^+W^-$ and were able to establish good high-energy behaviour for each individual square or

interference term of the three contributing Feynman diagrams.

In this paper we will apply similar methods in order to isolate the W-fusion part of the $qq \to qqZ$ process in the form of a squared subamplitude that is both gauge independent and respects unitarity. This subamplitude squared can then be used to provide a well-defined approximation to Higgs production based only on W-fusion that, as we shall see, works particularly well in the region of the resonance and above. It should therefore provide a useful analysis tool for simulating Higgs production at, for example, the LHC pp collider, especially in a Monte Carlo context where the compactness of our expressions for the subamplitude avoids a time consuming calculation of the full amplitude.

The paper is in essentially two parts. In the following section we discuss in some detail how to implement the pinch technique in the context of the W-fusion process. Having arrived at the final expressions for the approximate scattering amplitude squared, we then perform numerical studies to compare our results for various distributions with those obtained from the full calculation. Our conclusions are presented in a final section.

2 A unitarity respecting amplitude for off-shell W fusion

In this section we will consider in detail the process

$$\bar{u}(q_1)u(q_2) \to \bar{d}(q_3)d(q_4)Z(k_1)Z(k_2) \tag{2.1}$$

which obviously can proceed via W- fusion. We will show how it is possible to isolate the W-fusion part of this process in a well defined way, and arrive at a squared amplitude that is gauge independent and respects unitarity.

The complete set of Feynman diagrams for this process exhibits a plethora of different propagators, and we can use these to classify the various types of diagrams. First, we separate all graphs into two categories according to whether the initial quarks annihilate (S graphs) or not (T graphs). The T graphs are those that contain t-channel W propagators. There are in total 34 T graphs (in the Feynman gauge) and we may further separate them according to their fermion propagator structure or, equivalently, according to the particles that emit the final-state Z bosons. Thus if we require both Zs to be emitted from gauge bosons, we obtain the usual six W-fusion graphs. These will be denoted collectively by T_{WW}

$$T_{WW} = T_W + T_{cW} + T_{4G} + T_\phi + T_{c\phi} + T_H \tag{2.2}$$

and are depicted in Fig. 1. Their characteristic feature is that they do not contain any fermion propagators. In fact their structure is described by

$$T_{WW} = \frac{V_\alpha}{W_1}\frac{U_\beta}{W_2} T_{WW}^{\alpha\beta\mu\nu}\epsilon_1^\mu \epsilon_2^\nu \ , \tag{2.3}$$

where W_1 and W_2 are the inverse propagators of the two *off-shell* W bosons given in (1.2). The external fermions only enter through the two fermion currents

$$V_\alpha = \frac{g}{\sqrt{2}}\overline{v}_u(q_1)\gamma_\alpha P_L v_d(q_3) \tag{2.4}$$

$$U_\beta = \frac{g}{\sqrt{2}}\overline{u}_d(q_4)\gamma_\beta P_L u_u(q_2) \ . \tag{2.5}$$

In the Feynman gauge the individual graphs are given explicitly by

$$T_W^{\alpha\beta\mu\nu} = \frac{c_W^2}{D_1}\ \Gamma^{\alpha\rho\mu}(p_1, k_1 - p_1, -k_1) \times\Gamma^{\beta\rho\nu}(p_2, k_2 - p_2, -k_2) \tag{2.6}$$

$$T_{cW}^{\alpha\beta\mu\nu} = \frac{c_W^2}{D_2}\ \Gamma^{\alpha\rho\nu}(p_1, k_2 - p_1, -k_2) \times\Gamma^{\beta\rho\mu}(p_2, p_2, k_1 - p_2, -k_1) \tag{2.7}$$

$$T_{4G}^{\alpha\beta\mu\nu} = c_W^2 \times G^{\alpha\beta\mu\nu}(p_1, p_2, k_1, k_2) \tag{2.8}$$

$$T_\phi^{\alpha\beta\mu\nu} = \frac{M_Z^2 s_W^4}{D_1}\ g^{\alpha\mu}g^{\beta\nu} \tag{2.9}$$

$$T_{c\phi}^{\alpha\beta\mu\nu} = \frac{M_Z^2 s_W^4}{D_2}\ g^{\alpha\nu}g^{\beta\mu} \tag{2.10}$$

$$T_H^{\alpha\beta\mu\nu} = \frac{M_Z^2}{D_H} g^{\alpha\beta}g^{\mu\nu} \tag{2.11}$$

where an overall factor of $(-ig^2)$ has been omitted from all graphs.

The kinematics of the process is described in Fig. 1, i.e.

$$p_1 = q_1 - q_3 \ , \qquad p_2 = q_2 - q_4 \ , \qquad p_1 + p_2 = k_1 + k_2 = q \ . \tag{2.12}$$

The inverse bosonic propagators appearing in these graphs are

$$D_1 = (k_1 - p_1)^2 - M_W^2 = (k_2 - p_2)^2 - M_W^2 \ , \tag{2.13}$$

$$D_2 = (k_1 - p_2)^2 - M_W^2 = (k_2 - p_1)^2 - M_W^2 \ , \tag{2.14}$$

$$D_H = q^2 - M_H^2 \ . \tag{2.15}$$

Note that an imaginary part must be included in the Higgs propagator D_H in order to regulate it when $q^2 = M_H^2$. We will comment on its precise form later. The t-channel propagators of the Ws will always be spacelike (< 0). In fact for the two Ws emitted from the external fermions we have

$$p_1^2 = -\frac{\sqrt{s}E_3}{2}(1 - \cos\theta_{13}) \ , \quad p_2^2 = -\frac{\sqrt{s}E_4}{2}(1 - \cos\theta_{24}) \ , \tag{2.16}$$

where the energies and scattering angles refer to the centre-of-mass frame. Thus the Ws will always be *off-shell* by at least an amount equal to their mass, $|W_1|, |W_2| \geq M_W^2$, with the minimum being attained for forward scattering, $\theta_{13} = 0 = \theta_{24}$ ($\Rightarrow\ p_1^2 = 0 = p_2^2$).

The forms of the trilinear $Z_\mu W_\alpha^- W_\beta^+$ and quadrilinear $Z_\mu Z_\nu W_\alpha^- W_\beta^+$ gauge boson vertices that appear in these

graphs are given, respectively, by

$$\Gamma_{\mu\alpha\beta}(q,p_1,p_2) = (q-p_1)_\beta g_{\mu\alpha} + (p_1-p_2)_\mu g_{\alpha\beta} + (p_2-q)_\alpha g_{\beta\mu} \ , \quad (2.17)$$

$$G_{\alpha\beta\mu\nu}(p_1,p_2,k_1,k_2) = 2g_{\alpha\beta}g_{\mu\nu} - g_{\alpha\mu}g_{\beta\nu} - g_{\alpha\nu}g_{\beta\mu} \ , \quad (2.18)$$

where all momenta are considered incoming.

The case where one Z is emitted from a fermion line while the other is emitted from a W is described by the eight graphs denoted by T_{Wf}:

$$T_{Wf} = T_{1d}+T_{1u}+T_{2d}+T_{2u}+T_{1\bar{d}}+T_{1\bar{u}}+T_{2\bar{d}}+T_{2\bar{u}} \ , \quad (2.19)$$

and depicted in Fig. 2. These graphs contain one fermion propagator and one trilinear gauge boson vertex. Only one of the currents V_α or U_β appears. A typical T_{Wf} graph has the following structure:

$$T_{1d} = \frac{V_\alpha}{W_1}\frac{1}{D_1}\Gamma_{\alpha\rho\mu}(p_1,k_1-p_1,-k_1)\ell_d \times \frac{g}{\sqrt{2}}\overline{u}_d\gamma_\nu P_L \frac{1}{\not q_2 - (\not k_1 - \not p_1)}\gamma^\rho u_u \epsilon_1^\mu \epsilon_2^\nu \ . \quad (2.20)$$

The couplings of the fermions to the Z are defined here as

$$\frac{ig}{c_w}\gamma^\mu\left(\ell_f P_L + r_f P_R\right) \quad (2.21)$$

where

$$\ell_f = I^3_{W,f} - s_w^2 Q_f, \qquad r_f = -s_w^2 Q_f \ . \quad (2.22)$$

In the above expressions $I^3_{W,f}$ is the third component of the weak isospin, Q_f the charge of fermion f, and $P_{R,L} = (1 \pm \gamma_5)/2$.

The remainder of the T graphs, where *both* Zs emanate from fermions, are denoted T_{ff} and are exhibited in Fig. 3:

$$T_{ff} = T_{W_1} + T_{W_2} + T_{D_1} + T_{D_2} \ . \quad (2.23)$$

Each one of these graphs contains two fermion propagators. In (2.23) we have grouped them according to the W propagator they contain. In this class of graphs either one current appears and two fermionic propagators are present in the other fermion line (T_{W_1} and T_{W_2} graphs, 6 graphs each), or no current appears and each fermion line contains one fermion propagator (T_{D_1} and T_{D_2} graphs, 4 graphs each). Altogether there are 20 graphs in this class.

Finally, the S graphs are divided into classes according to the neutral gauge boson (γ, Z, or g) into which the initial quarks anihilate. There are 63 graphs in this category, denoted as S_Z (20), S_γ (20), S_g (20), and S_{ZZ} (3) according to the gauge boson propagators that they contain. In the S_V graphs the Zs are emitted from fermions and thus all these graphs contain two fermion propagators. The S_{ZZ} graphs are the Higgs-strahlung graphs. Like the W fusion graphs they contain no fermion propagators. One representative of each of these classes is shown in Fig. 4.

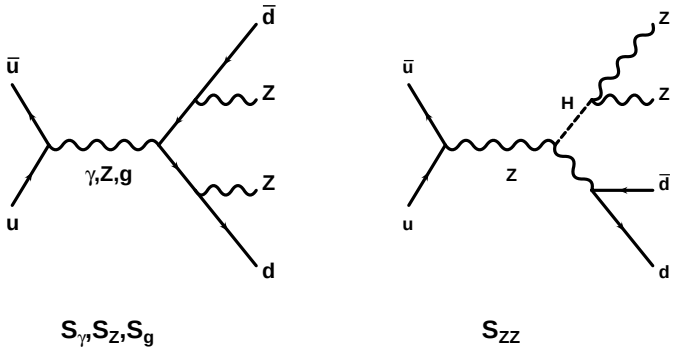

Fig. 4. The S graphs. There are 20 S_g, S_γ and S_Z graphs respectively. One of the three Higgs-strahlung graphs is also shown

These seemingly different classes of graphs contain in fact a large number of identical terms. These common terms are responsible for the large unitarity cancellations that take place in the sum of all graphs. On the other hand, unitarity violation occurs within individual subsets of graphs, e.g. T_{WW}, as a result of incomplete cancellations among such terms. The common terms among the different classes of graphs arise when momentum factors in the graphs' numerators trigger one of the following tree-level Ward identities:

$$k^\mu\gamma_\mu \equiv \not k = (\not k + \not q_i) - \not q_i = S^{-1}(k+q_i) - S^{-1}(q_i), \quad (2.24)$$

$$q^\mu\Gamma_{\mu\alpha\beta}(q,p_1,p_2) = [p_2^2 g_{\alpha\beta} - p_{2\alpha}p_{2\beta}] - [p_1^2 g_{\alpha\beta} - p_{1\alpha}p_{1\beta}] = U^{-1}_{\alpha\beta}(p_2)_W - U^{-1}_{\alpha\beta}(p_1)_W, \quad (2.25)$$

$$k_1^\mu G_{\alpha\beta;\mu\nu}(p_1,p_2;k_1,k_2) = \Gamma_{\alpha\beta\nu}(p_1,p_2+k_1,k_2) - \Gamma_{\alpha\beta\nu}(p_1+k_1,p_2,k_2), \quad (2.26)$$

$$k_1^\mu k_2^\nu g_{\mu\nu} = \frac{1}{2}(q^2 - k_1^2 - k_2^2) = \frac{1}{2}D_H + \frac{1}{2}(M_H^2 - 2M_Z^2), \quad (2.27)$$

where (2.27) is the Ward identity of the HZZ vertex with the two Z bosons on shell, while $U^{-1}_{\alpha\beta}(p)_W = (p^2 - M_W^2)g_{\alpha\beta} - p_\alpha p_\beta$ is the inverse propagator of the W in the unitary gauge. The inverse propagators generated in this way cancel one of the propagators of the graph, resulting in a structure that mimics the structure of a different class. For example, the two classes of graphs WW and Wf become identical in form when one of the W_i propagators is removed in the T_{WW} graphs while at the same time the fermion propagator is removed in the T_{Wf} graphs. The remaining terms in the Ward identities mostly cancel when the particles involved are on shell. As we have already noted, the momentum factors in the numerators that trigger the above Ward identities are furnished by the trilinear gauge boson vertices and the longitudinal polarization vectors of the external Z bosons. In fact current conservation, good high energy behaviour, the equivalence theorem and the cancellation of gauge parameters all have

their origins in these and other similar Ward identities satisfied by the tree-level vertices of the Standard Model. Indeed a set of tree-level graphs is characterised as gauge invariant when none of its parts can resemble the structure of a different set of graphs by use of a Ward identity.

With this criterion in mind it should now be clear that the S graphs are not involved in any unitarity cancellations with the T graphs. First of all the couplings involved are different. For example the S_g graphs can never mix with any other class of graphs since they are the only ones that involve the strong coupling constant. Thus they are gauge invariant and well behaved by themselves. Second, there are not enough factors in the numerators of these two classes that are capable of cancelling the necessary propagators to make a common term. One W propagator will always survive in the T graphs while no such propagator is present in the S graphs. Thus in the search for a well behaved W-fusion squared amplitude the S graphs can be ignored, and we need only concentrate on the T graphs.

With these considerations it should also be evident that *off-shell* Z-fusion or Higgs-strahlung cannot give rise to unitarity violation [2]. The Higgs-strahlung graphs S_{ZZ} cannot communicate in any way with the rest of the graphs. Even if their Higgs propagator is cancelled they will always contain two Z boson propagators.

Equivalently the good high energy behaviour of the T graphs alone can also be verified by considering a different W-fusion process where the initial fermions cannot annihilate, like $e^+\mu^- \to \nu\bar{\nu}_\mu ZZ$. This process still retains the T graphs but does not involve any S graphs.

The Ward identities of (2.24-2.27) guarantee both the gauge parameter independence of the amplitude as well as independence with respect to gauge transformations of the external gauge bosons. For physical amplitudes with external gauge bosons, gauge invariance is encoded in the following relationships:

$$\gamma; g: \quad k^\mu T_\mu(\gamma; g) = 0 \tag{2.28}$$

$$W^\pm: \quad k^\mu T_\mu(W^\pm) = \pm M_W \mathcal{T}(\phi) \tag{2.29}$$

$$Z: \quad k^\mu T_\mu(Z) = -iM_Z \mathcal{T}(\chi) \tag{2.30}$$

In these equations $T_\mu(\gamma; g)$, $T_\mu(W^\pm)$, $T_\mu(Z)$ are physical amplitudes with at least one external gauge boson γ, g, $W^\pm$, Z carrying momentum k^μ. The amplitudes $\mathcal{T}(\phi)$ and $\mathcal{T}(\chi)$ on the right-hand side are the corresponding set of graphs where the gauge boson is replaced by its would-be Goldstone boson. The above (2.28-2.30) can be considered as Ward identities for whole set of graphs and they are the direct consequence of the Ward identities of (2.24-2.27)A set of graphs that satisfies these Ward identities is said to be gauge invariant. It would be both independent of any gauge parameters and of the choice of polarization vector for the external gauge boson. For the photon, (2.28) is usually referred to as current conservation in QED, while from (2.29) and (2.30) the Equivalence Theorem follows directly [8].

In our case, since the fermions are massless and there is no χWW vertex, the T_{Wf} and T_{ff} graphs will give no contribution to the right-hand side of (2.30). Thus

$$k_1^\mu T_\mu(Z) = -iM_Z \mathcal{T}_{WW}(\chi)\ . \tag{2.31}$$

Since unitarity in *off-shell* W-fusion is violated by terms which are proportional to the *off-shellness* of the W bosons [2], the common terms between the T_{WW} and the $T_{Wf} + T_{ff}$ graphs will always be proportional to W_1 and W_2. In the calculation of the squared amplitude such common terms will emerge at three different levels. The first level is that of the amplitude, stripped of the polarization vectors of the Zs

$$T^{\mu\nu} = (T_{WW} + T_{Wf} + T_{ff})^{\mu\nu}\ . \tag{2.32}$$

At this level, the presence of the trilinear vertices already generates *off-shell* unitarity violating terms in the T_{WW} and T_{Wf} that cancel between them. At this stage all gauge parameters cancel also.

The second cancellation occurs when in the full amplitude,

$$T = T^{\mu\nu}\epsilon_1^\mu \epsilon_2^\nu\ , \tag{2.33}$$

the polarization vectors of the Z bosons become longitudinal and thus their leading part becomes proportional to the momenta of the Zs, k_1^μ and k_2^ν. Now the action of k_1^μ and/or k_2^ν on the amplitude will produce extra *off-shell* terms. Such terms will again cancel among the T_{WW} and $T_{Wf} + T_{ff}$ graphs.

Finally, in the squared amplitude additional *off-shell* terms will appear between the squared W-fusion amplitude $|T_{WW}|^2$ and the interference term $T_{WW}(T^*_{Wf} + T^*_{ff})$. Most of these terms again cancel. Those that do not, emerge from the interferences of the Higgs graph T_H. Because of their structure (they contain no fermion propagators), these terms will be allocated to the W-fusion amplitude $|T_{WW}|^2$.

Accounting for these cancellations at every level is simply an exercise in identifing structures. The common terms can actually be identified graphically, as in Fig. 5 or Fig. 6. In order to keep track of them the properties and the Ward identities of the gauge boson self-interaction vertices are exploited. Thus the trilinear gauge vertex of (2.17) is decomposed in the asymmetric form, first used by t' Hooft [6],

$$\Gamma_{\mu\alpha\beta}(q, p_1, p_2) = \Gamma^F_{\mu\alpha\beta}(q; p_1, p_2) + \Gamma^P_{\mu\alpha\beta}(q; p_1, p_2)\ , \tag{2.34}$$

where

$$\Gamma^F_{\mu\alpha\beta}(q; p_1, p_2) = (p_1 - p_2)_\mu g_{\alpha\beta} - 2q_\alpha g_{\beta\mu} + 2q_\beta g_{\mu\alpha} \tag{2.35}$$

$$\Gamma^P_{\mu\alpha\beta}(q; p_1, p_2) = -p_{1\alpha} g_{\beta\mu} + p_{2\beta} g_{\mu\alpha}\ . \tag{2.36}$$

The pinch part is proportional to the momenta of two of the legs of the vertex carrying their corresponding Lorentz index. This part therefore vanishes identically when the two legs are on shell. The Γ^F part of the vertex satisfies the Feynman gauge part of the Ward identity of (2.25),

$$q^\mu \Gamma^F_{\mu\alpha\beta}(q; p_1, p_2) = (p_2^2 - p_1^2) g_{\alpha\beta} = (W_2 - W_1) g_{\alpha\beta}\ , \tag{2.37}$$

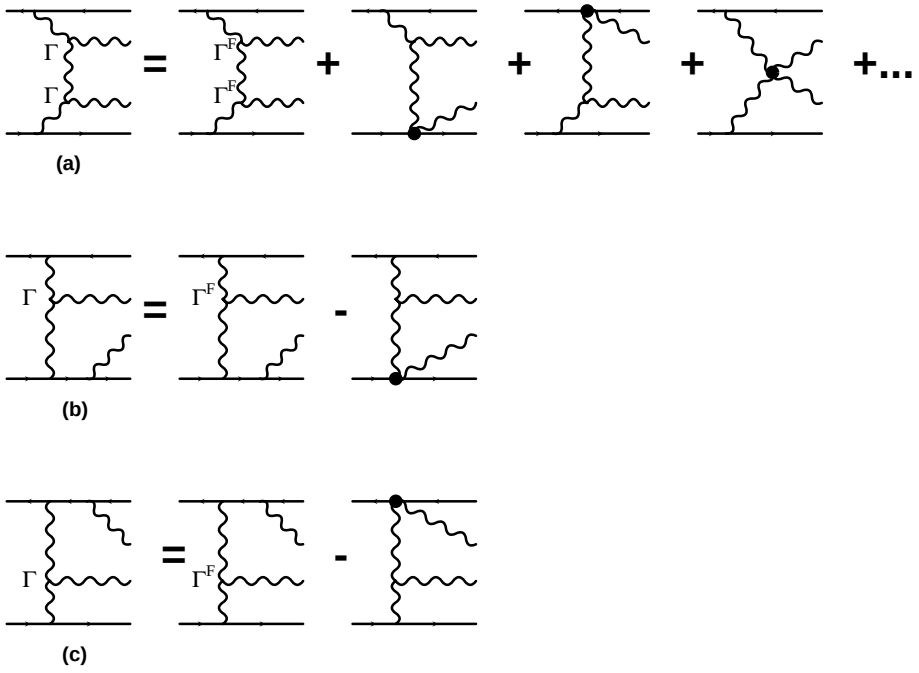

Fig. 5. Pinch terms induced by the presence of the trilinear gauge vertices

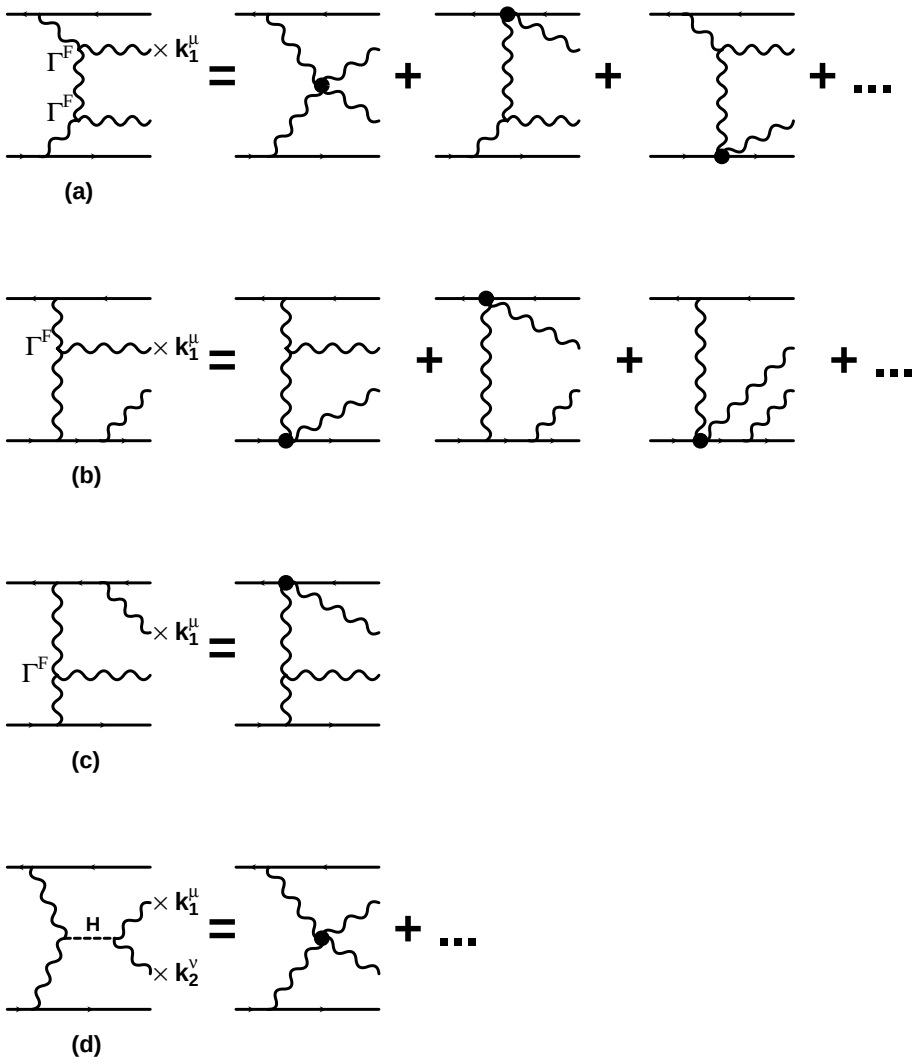

Fig. 6. Pinch terms induced by the momentum of a longitudinal Z boson. The sum of (a), (b), (c) and the relevant term for the T_{ff} graphs is a pictorial representation of the Ward Identity of (2.30) when the trilinear vertices in the graphs are the full ones. In the sum, all pinch terms on the r.h.s. cancel and the remainder equals the graphs $\mathcal{T}(\chi)$, with the external Z replaced by its would-be Goldstone boson χ. Terms represented by the ellipsis on the r.h.s. of (b) contribute to the remainder R_1^ν of (2.77). In (d) we show how pinching is induced in the Higgs graph according to the Ward identity of (2.27). The pinch term on the r.h.s. contributes to the $g_{\alpha\beta}$ term of F_1 in (2.83)

while the pinch part Γ^P will give rise to the longitudinal terms of (2.25). The four-gauge-boson vertex of (2.18) can also be split into two parts:

$$G_{\alpha\beta;\mu\nu}(p_1,p_2;-k_1,-k_2) = G^F_{\alpha\beta;\mu\nu}(p_1,p_2;-k_1,-k_2) + G^P_{\alpha\beta;\mu\nu}(p_1,p_2;-k_1,-k_2)\ , \quad (2.38)$$

$$G^F_{\alpha\beta;\mu\nu}(p_1,p_2;-k_1,-k_2) = 2g^{\alpha\beta}g^{\mu\nu}\ , \quad (2.39)$$

$$G^P_{\alpha\beta;\mu\nu}(p_1,p_2;-k_1,-k_2) = -g^{\alpha\mu}g^{\beta\nu} - g^{\alpha\nu}g^{\beta\mu}\ . \quad (2.40)$$

With the above decomposition, the Ward identity of (2.26) is also satisfied individually by its Feynman (G^F) and pinch (G^P) parts.

We next proceed to explicitly exhibit and implement the aforementioned cancellations between the W-fusion and the rest of the T graphs. Most of the remaining part of this section will be quite technical, involving extended use of the relevant Ward identities. Readers who are only interested in the results of the calculation may wish to go directly to (2.92) and the discussion that follows it.

The 1st cancellation

In order to identify the common *off-shell* terms at this level one must first decompose the trilinear and quadrilinear gauge vertices into their Feynman and pinch parts. The two sets of graphs T_{WW} and T_{Wf} which contain such vertices will then separate into Feynman and pinch parts respectively:

$$T^{\mu\nu}_{WW} = T^{F\mu\nu}_{WW} + T^{P\mu\nu}_{WW}\ ,$$
$$T^{\mu\nu}_{Wf} = T^{F\mu\nu}_{Wf} + T^{P\mu\nu}_{Wf}\ . \quad (2.41)$$

The pinch parts are proportional to the *off-shellness* of the W bosons. We will explicitly show that these parts exactly cancel.

Since the decomposition of a trilinear vertex in (2.34) is asymmetric, at this point one has to make a choice for the first momentum argument of the Γ^F vertices. Different choices should make no difference to the final result when the procedure is carried through consistently. Nevertheless at intermediate points a particular choice may facilitate the calculations. It turns out that choosing as the special momentum for the Γ^F vertices the momentum of the corresponding off-shell W, $p_{1\alpha}$ or $p_{2\beta}$, minimizes the number of interference terms that must be considered, thus expediting the calculations.[2] Thus the Feynman and pinch parts of the vertices are:

$$\Gamma^F_{\alpha\rho\mu}(p_1;k_1-p_1,-k_1) = 2(k_{1\alpha}g_{\rho\mu} + p_{1\mu}g_{\alpha\rho} - p_{1\rho}g_{\mu\alpha})\ ;$$
$$\Gamma^P_{\alpha\rho\mu}(p_1;k_1-p_1,-k_1) = (p_1-k_1)_\rho g_{\mu\alpha} \quad (2.42)$$

$$\Gamma^F_{\beta\rho\nu}(p_2;k_2-p_2,-k_2) = 2(k_{2\beta}g_{\rho\nu} + p_{2\nu}g_{\beta\rho} - p_{2\rho}g_{\nu\beta})\ ;$$
$$\Gamma^P_{\beta\rho\nu}(p_2;k_2-p_2,-k_2) = (p_2-k_2)_\rho g_{\nu\beta} \quad (2.43)$$

[2] Actually this choice is identical to the one made in the one-loop pinch technique, since these would be the momenta outside the loop in $WW \to ZZ$.

$$\Gamma^F_{\alpha\rho\nu}(p_1;k_2-p_1,-k_2) = 2(k_{2\alpha}g_{\rho\nu} + p_{1\nu}g_{\alpha\rho} - p_{1\rho}g_{\nu\alpha})\ ;$$
$$\Gamma^P_{\alpha\rho\nu}(p_1;k_2-p_1,-k_2) = (p_1-k_2)_\rho g_{\nu\alpha} \quad (2.44)$$

$$\Gamma^F_{\beta\rho\mu}(p_2;k_1-p_2,-k_1) = 2(k_{1\beta}g_{\rho\mu} + p_{2\mu}g_{\beta\rho} - p_{2\rho}g_{\mu\beta})\ ;$$
$$\Gamma^P_{\beta\rho\mu}(p_2;k_1-p_2,-k_1) = (p_2-k_1)_\rho g_{\mu\beta} \quad (2.45)$$

In the above expressions we have dropped all terms that will not contribute to the matrix element. These are the terms proportional to $p_{1\alpha}$ and $p_{2\beta}$, which for massless fermions vanish when contracted with the external fermionic currents, i.e. $p_{1\alpha}V^\alpha = 0$ and $p_{2\beta}U^\beta = 0$. Furthermore at this level we can also drop terms proportional to $k_{1\mu}$ and $k_{2\nu}$ that vanish when contracted with the polarization vectors of the Zs: $k_{1\mu}\epsilon^\mu(k_1) = 0 = k_{2\nu}\epsilon^\nu(k_2)$.

It is straightforward to calculate the pinch part of the T_{Wf} graphs. Since they contain only one trilinear vertex they split immediately into two parts. One readily observes that the pinch part, Γ^P, of the vertex simply cancels the fermion propagator in each of these graphs by virtue of the Ward identity of (2.24). We illustrate this explicitly for one of the graphs. The expression for T_{1d} of Fig. 2 has already been written out explicitly in (2.20). Using (2.42) for $\Gamma^P_{\beta\rho\nu}$, the pinch part of this graph is given by

$$T^P_{1d} = \frac{V^\alpha}{W_1}\frac{g_{\alpha\mu}}{D_1}\frac{g}{\sqrt{2}}\ell_d\bar{u}_d\gamma_\nu\frac{1}{\not q_2 - \not k_1 + \not p_1} \times(\not p_1 - \not k_1)P_L u_u(q_2)\epsilon_1^\mu\epsilon_2^\nu\ . \quad (2.46)$$

Then writing

$$\not p_1 - \not k_1 = (\not q_2 - \not k_1 + \not p_1) - \not q_2\ , \quad (2.47)$$

the first term will cancel the fermion propagator while the second one vanishes since $\not q_2 u_u(q_2) = 0$. So the pinch part of this graph is

$$T^P_{1d} = \frac{V^\alpha}{W_1}\frac{U^\beta}{W_2}(\ell_d)\frac{W_2}{D_1}g_{\alpha\mu}g_{\beta\nu}\epsilon_1^\mu\epsilon_2^\nu\ . \quad (2.48)$$

The corresponding expression T^P_{1u}, of graph T_{1u} of Fig. 2 is simply obtained by (i) changing ℓ_d, the fermion coupling of the Z, to ℓ_u since the Z boson is now emitted from the *up* fermion, and (ii) changing the overall sign, since now the fermion propagator involves $\not q_3 - (\not p_1 - \not k_1)$. Thus, using the following relation for the fermion couplings,

$$\ell_u - \ell_d = c_w^2\ , \quad (2.49)$$

the two graphs combined give

$$T^P_1 \equiv T^P_{1u} + T^P_{1d} = \frac{V_\alpha}{W_1}\frac{U_\beta}{W_2}(-c_w^2)\frac{W_2}{D_1}g_{\alpha\mu}g_{\beta\nu}\ . \quad (2.50)$$

Evidently this expression resembles the structure of the W-fusion graphs, T_{WW}. It contains no fermion propagators and has the correct coupling. We have divided and multiplied by the W boson inverse propagator W_2 in order to bring the expression into the form of (2.3). This step is not strictly necessary, but our convention will be

always to extract a factor $V_\alpha U_\beta/(W_1 W_2)$ from all such terms.

The pinch parts of the rest of the T_{Wf} graphs are extracted in a similar way. The graphs always combine in pairs to produce the correct coupling c_w^2. Altogether we obtain for the pinch terms of the T_{Wf} graphs the following expression:

$$T_{Wf}^P = \frac{V_\alpha}{W_1}\frac{U_\beta}{W_2}(-c_w^2)(W_1+W_2)\{\frac{g_{\alpha\mu}g_{\beta\nu}}{D_1}+\frac{g_{\alpha\nu}g_{\beta\mu}}{D_2}\}\epsilon_1^\mu\epsilon_2^\nu \ . \tag{2.51}$$

Next we turn to the W-fusion graphs. In order to identify similar pinch terms to those of the T_{Wf} graphs we will use the following identity for the product of two trilinear vertices [7]:

$$\Gamma_{\alpha\rho\mu}\Gamma_{\beta\rho\nu} = \Gamma^F_{\alpha\rho\mu}\Gamma^F_{\beta\rho\nu}+\Gamma^P_{\alpha\rho\mu}\Gamma_{\beta\rho\nu}+\Gamma_{\alpha\rho\mu}\Gamma^P_{\beta\rho\nu}-\Gamma^P_{\alpha\rho\mu}\Gamma^P_{\beta\rho\nu} \ . \tag{2.52}$$

This decomposition will enable us to make use of the Ward identity of the full vertex given in (2.25).

Let us first consider the graph T_W given in (2.6). Using (2.52), the product of its trilinear vertices can be expressed as

$$\begin{aligned}&\Gamma_{\alpha\rho\mu}(p_1,k_1-p_1,-k_1)\Gamma_{\beta\rho\nu}(p_2,k_2-p_2,-k_2)\\ &\quad=\Gamma^F_{\alpha\rho\mu}(p_1;k_1-p_1,-k_1)\Gamma^F_{\beta\rho\nu}(p_2;k_2-p_2,-k_2)\\ &\quad+g_{\beta\nu}(p_2-k_2)_\rho\Gamma^{\alpha\rho\mu}(p_1,k_1-p_1,-k_1)\\ &\quad+g_{\alpha\mu}(p_1-k_1)_\rho\Gamma^{\beta\rho\nu}(p_2,k_2-p_2,-k_2)\\ &\quad-g_{\alpha\mu}g_{\beta\nu}(p_2-k_2)\cdot(p_1-k_1) \ .\end{aligned} \tag{2.53}$$

Since $p_1-k_1=k_2-p_2$, the Ward identity of (2.25) is immediately triggered by the second and third term of the above equation. This will produce *off-shell* terms proportional to $p_i^2=W_i+M_W^2$. The fourth term can be written in terms of the inverse propagator D_1 when M_W^2 is added and subsequently subtracted. Finally, using the on-shell condition for the Zs, $k_1^2=k_2^2=M_Z^2$, the expression (2.6) for the diagram T_W is transformed into

$$\begin{aligned}T_W^{\alpha\beta\mu\nu} = \frac{c_w^2}{D_1}\big[&\Gamma^F_{\alpha\rho\mu}\Gamma^F_{\beta\rho\nu}+[M_Z^2(c_w^2-2s_w^2)\\ &+D_1+(W_1+W_2)]g_{\alpha\mu}g_{\beta\nu}\big] \ .\end{aligned} \tag{2.54}$$

The momenta arguments of the vertices will no longer be exhibited, since the way their momenta are assigned should be obvious from the Lorentz indices of the vertices. The first and third indices determine the first and third momentum arguments of the vertex respectively, according to $(\mu,\nu,\alpha,\beta)\to(-k_1,-k_2,p_1,p_2)$, while the second argument is fixed by momentum conservation. In an identical way the crossed graph T_{cW} is rewritten as

$$\begin{aligned}T_{cW}^{\alpha\beta\mu\nu} = \frac{c_w^2}{D_2}\big[&\Gamma^F_{\alpha\rho\nu}\Gamma^F_{\beta\rho\mu}+[M_Z^2(c_w^2-2s_w^2)\\ &+D_2+(W_1+W_2)]g_{\alpha\nu}g_{\beta\mu}\big]\end{aligned} \tag{2.55}$$

Having obtained these new forms for the diagrams T_W and T_{cW} we make the following observations. The terms proportional to $M_Z^2(c_w^2-2s_w^2)$, directly combine with the corresponding would-be Goldstone graphs of (2.9) and (2.10) to produce an overall coupling equal to $s_w^4-2s_w^2c_w^2+c_w^4=(c_w^2-s_w^2)^2$. The terms proportional to D_1 or D_2 will immediately cancel the relevant propagator of the graph, i.e. either $1/D_1$ or $1/D_2$, and will thus combine with the quadrilinear vertex graph T_{4G}. In doing so they cancel the G^P pinch part of the quadrilinear vertex. The last terms proportional to the *off-shellness* of the W bosons are the pinch terms. These operations are represented pictorially for graph T_W in Fig. 5(a), where the ellipsis represent the $M_Z^2(c_w^2-2s_w^2)$ term of (2.54)

Thus the Feynman and pinch parts of the T_{WW} graphs are given by the following expressions:

$$\begin{aligned}T_{WW}^{F\mu\nu} = \frac{V_\alpha}{W_1}\frac{U_\beta}{W_2}\Big\{&\frac{c_w^2}{D_1}\Gamma^F_{\alpha\rho\mu}\Gamma^F_{\beta\rho\nu}+\frac{c_w^2}{D_2}\Gamma^F_{\alpha\rho\nu}\Gamma^F_{\beta\rho\mu}\\ &+2c_w^2g_{\alpha\beta}g_{\mu\nu}+M_Z^2(c_w^2-s_w^2)^2[\frac{g_{\alpha\mu}g_{\beta\nu}}{D_1}\\ &+\frac{g_{\alpha\nu}g_{\beta\mu}}{D_2}]+M_Z^2\frac{g_{\alpha\beta}g_{\mu\nu}}{D_H}\Big\} \ ,\end{aligned} \tag{2.56}$$

and

$$T_{WW}^{P\mu\nu} = \frac{V_\alpha}{W_1}\frac{U_\beta}{W_2}(c_w^2)(W_1+W_2)\{\frac{g_{\alpha\mu}g_{\beta\nu}}{D_1}+\frac{g_{\alpha\nu}g_{\beta\mu}}{D_2}\} \ . \tag{2.57}$$

We note that the *off-shell* pinch terms have only been generated from the graphs that contain trilinear gauge vertices, namely T_W and T_{cW}. Only these two graphs can communicate with the rest of the graphs, in this case T_{Wf}, due to the rich momentum structure of their numerator.

Finally we observe that the pinch part of the W-fusion graphs, $T_{WW}^{P\mu\nu}$ in the above equation, exactly cancels the pinch term of the T_{Wf} graphs T_{Wf}^P of (2.51). Indeed

$$T_{WW}^P+T_{Wf}^P=0 \ . \tag{2.58}$$

We have also verified the above results by performing the calculations in a general R_ξ gauge. For this $2\to4$ process the cancellation of the gauge parameters due to current conservation is not automatic as in the case of a $2\to2$ process. Common pinch terms among different classes of graphs are now even more prolific, due to the presence of the extra momenta in the longitudinal part of the gauge bosons' propagators. In addition, most of them will also be gauge parameter dependent. When all such terms are identified and cancelled the surviving expressions coincide with those obtained in the Feynman gauge. Thus the formula of (2.56) for T_{WW}^F and the corresponding ones for T_{Wf}^F and T_{ff} are truly gauge parameter independent expressions.

It would be interesting to find or invent a gauge where these expressions could be obtained *automatically* by the Feynman rules of the particular gauge. In such a gauge this first level of cancellations would be avoided. Furthermore such a gauge might prove useful in other multi-gauge-boson processes. However we are not aware of any such special gauge. Although the Γ^F vertices of (2.42–2.45) look similar to the trilinear vertices of the Gervais-Neveu

gauge [9], they are actually not the same, and thus the Gervais-Neveu gauge expression of the W-fusion graphs does not coincide with T^F_{WW}.

Although the expression for the W fusion graphs (2.56), obtained after this first step, is gauge parameter independent, it remains however gauge non-invariant in the sense that it still does not satisfy the Ward identity of (2.30). Because of this fact, the W fusion part can still not be separated from the rest of the graphs. To do this, the cancellations inherent in (2.30) must be allowed to take place first. This is done in the next step. We also note that the following steps would not be necessary had we considered photons instead of Zs in the final state, i.e. $WW \to \gamma\gamma$.

The 2nd cancellation

After this first cancellation has taken place the resulting gauge parameter independent amplitude T for our process can be written as

$$\begin{aligned} T &= (T^F_{WW} + T^P_{WW} + T^F_{Wf} + T^P_{Wf} + T_{ff})^{\mu\nu}\epsilon^\mu_1\epsilon^\nu_2 \\ &= (T^F_{WW} + T^F_{Wf} + T_{ff})^{\mu\nu}\epsilon^\mu_1\epsilon^\nu_2 \ . \end{aligned} \tag{2.59}$$

The further cancellations due to the longitudinal Z bosons become more transparent in the squared unpolarized amplitude where the sum over the polarizations of the Zs will give a factor

$$\sum_{\lambda_1} \epsilon^\mu_Z(k_1,\lambda_1)\epsilon^{*\mu'}_Z(k_1,\lambda_1) = -g_{\mu\mu'} + \frac{k^\mu_1 k^{\mu'}_1}{M^2_Z} \ , \tag{2.60}$$

and similarly for $\epsilon^\nu_Z(k_2,\lambda_2)$. The extra momentum factors, k^μ_1, k^ν_2 etc. introduced in this way will result in bad high energy behaviour, since their growth with energy cannot be compensated by the constant factors of M_Z in the denominator. Thus cancellations at this stage will be instrumental in restoring unitarity.

The unpolarized squared amplitude is given by

$$\begin{aligned} \overline{|T|^2} = \frac{1}{4} &T^{F\mu\nu}\big(-g_{\mu\mu'} + k_{1\mu}k_{1\mu'}/M^2_Z\big) \\ &\times \big(-g_{\nu\nu'} + k_{2\nu}k_{2\nu'}/M^2_Z\big)T^{F*}_{\mu'\nu'} \ . \end{aligned} \tag{2.61}$$

Expanding the product of polarization tensors gives four terms:

$$\begin{aligned} 4\,\overline{|T|^2} = &T^{F\mu\nu}T^{F*}_{\mu\nu} - \frac{k_{1\mu}}{M_Z}T^{F\mu\nu}\frac{k_{1\mu'}}{M_Z}T^{F*}_{\mu'\nu} \\ &-\frac{k_{2\nu}}{M_Z}T^{F\mu\nu}\frac{k_{2\nu'}}{M_Z}T^{F*}_{\mu\nu'} \\ &+\frac{k_{2\nu}k_{1\mu}}{M^2_Z}T^{F\mu\nu}\frac{k_{2\nu'}k_{1\mu'}}{M^2_Z}T^{F*}_{\mu'\nu'} \ . \end{aligned} \tag{2.62}$$

We next determine the effect of the factors of longitudinal momenta within each of the following terms:

$$k_{1\mu}T^{F\mu\nu}, \quad k_{2\nu}T^{F\mu\nu}, \quad \text{and} \quad k_{2\nu}k_{1\mu}T^{F\mu\nu} \ , \tag{2.63}$$

before actually squaring them. We will then explicitly show the generation and cancellation of the common *off-shell* terms within each of the above terms.

The action of k^μ_1 on the T_{WW} amplitudes will generate *off-shell* terms when contracted with the Γ^F vertices. Since k^μ_1 is not the first, special, argument of Γ^F the Feynman Ward identity of (2.37) is modified to:

$$k^\mu_1\Gamma^F_{\alpha\rho\mu} = \big(-D_1 + M^2_Z + W_1\big)\,g_{\alpha\rho} + 2k_{1\alpha}(k_1 - p_1)_\rho \tag{2.64}$$

for the graph T_W, and to

$$k^\mu_1\Gamma^F_{\beta\rho\mu} = \big(-D_2 + M^2_Z + W_2\big)\,g_{\beta\rho} + 2k_{1\beta}(k_1 - p_2)_\rho \tag{2.65}$$

for the crossed graph T_{cW}. The remaining terms $(k_1 - p_1)_\rho$ and $(k_1 - p_2)_\rho$ of the above equations will create additional *off-shell* terms when they act in turn on the remaining Γ^F vertex of each graph. Now the modified Ward identities read:

$$\begin{aligned} (k_1 - p_1)^\rho\Gamma^F_{\beta\rho\nu} &= -[D_1 + W_2 + M^2_Z(c^2_w - s^2_w)]g_{\beta\nu} \\ &\quad -2k_{2\beta}k_{2\nu} \ , \\ (k_1 - p_2)^\rho\Gamma^F_{\alpha\rho\nu} &= -[D_2 + W_1 + M^2_Z(c^2_w - s^2_w)]g_{\alpha\nu} \\ &\quad -2k_{2\alpha}k_{2\nu} \ , \end{aligned} \tag{2.66}$$

where the following elementary identities have been used for the dot products:

$$\begin{aligned} 2k_1\cdot p_1 &= -D_1 + M^2_Z + W_1 \ , \\ 2k_1\cdot p_2 &= -D_2 + M^2_Z + W_2 \ , \qquad (2.67) \\ 2k_2\cdot p_1 &= -D_2 + M^2_Z + W_1 \ , \\ 2k_2\cdot p_2 &= -D_1 + M^2_Z + W_2 \ . \qquad (2.68) \end{aligned}$$

In the end the contraction of k^μ_1 with the T^F_{WW} graphs assumes the following form:

$$k^\mu_1 T^{F\mu\nu}_{WW} = M^2_Z A^\nu_1 - 2c^2_w F_1 k^\nu_2 + M^2_Z\frac{F_2}{D_H}k^\nu_1 + c^2_w O^\nu_1 \ . \tag{2.69}$$

In the term A^ν_1 the index ν is never carried by either k_2 or k_1. The dependence on k^ν_2 or k^ν_1 has been explicitly exhibited, the latter emerging from the Higgs graph. The explicit expressions read:

$$\begin{aligned} A^\nu_1 = \frac{V^\alpha}{W_1}\frac{U^\beta}{W_2}\Bigg[&\frac{c^2_w}{D_1}\Gamma^F_{\beta\alpha\nu} + \frac{c^2_w}{D_2}\Gamma^F_{\alpha\beta\nu} - (2c^2_w - 1) \\ &\times\left(\frac{k^\alpha_1 g^{\beta\nu}}{D_1} + \frac{k^\beta_1 g^{\alpha\nu}}{D_2}\right)\Bigg] \end{aligned} \tag{2.70}$$

$$F_1 = \frac{V^\alpha}{W_1}\frac{U^\beta}{W_2}t^{\alpha\beta} \tag{2.71}$$

$$F_2 = \frac{V^\alpha}{W_1}\frac{U^\beta}{W_2}g^{\alpha\beta} \tag{2.72}$$

with

$$t^{\alpha\beta} = g^{\alpha\beta} + \frac{2k^\alpha_1 k^\beta_2}{D_1} + \frac{2k^\beta_1 k^\alpha_2}{D_2} \ . \tag{2.73}$$

The *off-shell* terms O_1 in (2.69) are

$$\begin{aligned} O^\nu_1 = \frac{V^\alpha}{W_1}\frac{U^\beta}{W_2}\Bigg[&\frac{W_1}{D_1}\Gamma^F_{\beta\alpha\nu} + \frac{W_2}{D_2}\Gamma^F_{\alpha\beta\nu} \\ &-2\frac{W_2}{D_1}k^\alpha_1 g^{\beta\nu} - 2\frac{W_1}{D_2}k^\beta_1 g^{\alpha\nu}\Bigg] \ . \end{aligned} \tag{2.74}$$

The action of k_1^μ on the T_{Wf} and T_{ff} graphs can be easily determined. Since mostly the Z bosons are emitted from fermion lines, the k_1^μ will directly pinch the fermion propagators adjacent to the Z boson leg by virtue of the Ward identity of (2.24) with $k \to k_1$.

When k_1^μ is emitted from a W then the modified Ward identities of (2.64) and (2.65) must be used. The terms $(k_1 - p_1)_\rho$ and $(k_1 - p_2)_\rho$ emerging from these identities will now pinch the fermion propagator attached to the internal W boson the same way as in (2.46). From the remaining terms of equations (2.64) and (2.65) the ones proportional to M_Z^2 cannot obviously pinch while the rest pinch one of the W propagators of the graphs. These latter pinch terms attain therefore a structure similar to that of the T_{ff} graphs and indeed will cancel exactly the entire contribution of the T_{ff} graphs.

After carrying out the above steps we finally obtain

$$k_1^\mu T_{Wf}^{F\mu\nu} = -c_w^2 O_1^\nu + M_Z^2 R_1^\nu - k_1^\mu T_{ff}^{\mu\nu} \ . \tag{2.75}$$

One immediately observes that the *off-shell* pinch terms that emerge from the T_{Wf} graphs are exactly opposite to the ones generated by the W-fusion graphs of (2.69) and exactly cancel. This is a manifestation of the Ward identity of (2.30). The remainder R_1^ν retains the structure of the T_{Wf} graphs and is given explictly by

$$\begin{aligned} R_1^\nu = \frac{V_\alpha}{W_1}\frac{1}{D_1}\frac{g}{\sqrt{2}}\overline{u}(q_4)\Big\{ & \ell_d\gamma^\nu \frac{1}{\not q_4 + \not k_2}\gamma^\alpha P_L \\ & + \ell_u \gamma^\alpha P_L \frac{1}{\not q_2 - \not k_2}\gamma^\nu \Big\} u(q_2) \\ + \frac{U_\beta}{W_2}\frac{1}{D_2}\frac{g}{\sqrt{2}}\overline{v}(q_1)\Big\{ & \ell_d\gamma^\beta P_L \frac{1}{\not q_3 + \not k_2}\gamma^\nu \\ & + \ell_u \gamma^\nu \frac{1}{\not q_1 - \not k_2}\gamma^\beta P_L \Big\} v(q_2) \ . \end{aligned} \tag{2.76}$$

Thus the action of k_1^μ on the complete amplitude will finally be of the form:

$$k_{1\mu} T^{\mu\nu} = M_Z^2 A_1^\nu - 2c_w^2 F_1 k_2^\nu + M_Z^2 \frac{F_2}{D_H} k_1^\nu + M_Z^2 R_1^\nu \ . \tag{2.77}$$

As already mentioned, this is nothing else but the Ward identity of (2.30) slightly modified by the remainder of the T_{Wf} graphs. The fact that such a term has survived in the left-hand side is simply because after the first cancellation the amplitudes have been written in terms of modified vertices Γ^F. Since we also do not contract with $\epsilon^\nu(k_2)$, the terms proportional to k_2^ν have also survived.

The effect of the longitudinal factor k_2^ν in the third term of (2.62) is obtained in an identical manner. As expected, the *off-shell* terms common between the T_{WW} and T_{Wf} graphs again cancel. In the end one obtains

$$k_{2\nu} T^{\mu\nu} = M_Z^2 A_2^\mu - 2c_w^2 F_1 k_1^\mu + M_Z^2 \frac{F_2}{D_H} k_2^\mu + M_Z^2 R_2^\mu \ , \tag{2.78}$$

where A_2^μ and R_2^μ can be obtained from (2.70) and (2.76) respectively by the replacements $k_1 \leftrightarrow k_2$ and $\mu \leftrightarrow \nu$.

Finally we examine the fourth term of (2.62), $k_{2\nu} k_{1\mu} T^{\mu\nu}$. Here the momenta of both Zs act on the amplitude. (The order in which the contractions are performed does not matter.) Acting first with k_1^μ again produces the result of (2.77). When next k_2^ν is contracted with this equation it generates *off-shell* terms from both classes of graphs. On the T_{WW} graphs it gives

$$k_2^\nu k_1^\mu T_{WW}^{F\alpha\beta\mu\nu} = M_Z^2 \left[(\frac{1}{2} - 4c_w^2) F_1 + A F_2 + c_w^2 O_{12} F_2 \right] \tag{2.79}$$

with

$$A = \left[\frac{M_W^2}{D_1} + \frac{M_W^2}{D_2} + \frac{M_H^2 - 2M_Z^2}{2D_H} \right] \tag{2.80}$$

and

$$O_{12} = \left[\frac{W_2}{D_1} + \frac{W_1}{D_2} \right] \ . \tag{2.81}$$

Here we have also used the Ward identity of the Higgs vertex, (2.27), to extract a piece from the Higgs graph and combine it with the gauge boson graphs in F_1.

The result for the remainder of the T_{Wf} graphs R_1^ν can be readily obtained by removing the fermionic propagators in (2.76) with $\not k_2$, by virtue of the Ward identity of (2.24). This gives

$$k_2^\nu R_1^\nu = -c_w^2 O_{12} F_2 \ . \tag{2.82}$$

Finally collecting together (2.79) and (2.82) we obtain

$$k_2^\nu k_1^\mu T^{\mu\nu} = M_Z^2 \left[(\frac{1}{2} - 4c_w^2) F_1 + F_2 A \right] \ . \tag{2.83}$$

Notice again that all *off-shell* terms have cancelled.

The 3rd cancellation

After the first two cancellations have taken place, the unpolarized squared amplitude of (2.62) attains the following form

$$\begin{aligned} 4\,\overline{|T|^2} = & \ T^{F\mu\nu} T_{\mu\nu}^{F*} \\ & - \frac{1}{M_Z^2}\left[M_Z^2 A_1^\nu - 2c_w^2 F_1 k_2^\nu + F_2 \frac{M_Z^2}{D_H} k_1^\nu + M_Z^2 R_1^\nu \right] \\ & \times \left[M_Z^2 A_1^\nu - 2c_w^2 F_1 k_2^\nu + F_2 \frac{M_Z^2}{D_H} k_1^\nu + M_Z^2 R_1^\nu \right]^* \\ & - \frac{1}{M_Z^2}\left[M_Z^2 A_2^\mu - 2c_w^2 F_1 k_1^\mu + F_2 \frac{M_Z^2}{D_H} k_2^\mu + M_Z^2 R_2^\mu \right] \\ & \times \left[M_Z^2 A_2^\mu - 2c_w^2 F_1 k_1^\mu + F_2 \frac{M_Z^2}{D_H} k_2^\mu + M_Z^2 R_2^\mu \right]^* \\ & + \left| (\frac{1}{2} - 4c_w^2) F_1 + F_2 A \right|^2 \ . \end{aligned} \tag{2.84}$$

We can now see the advantages of our choice for the Γ^F vertices. When each term of (2.84) is squared, additional *off-shell* terms will appear due to the interference of the

T_{WW} with the $T_{Wf}+T_{ff}$ graphs. This comes about from the action of the terms k_1^μ, k_2^ν, k_1^ν and k_2^μ which have been written explicitly in (2.84). No such terms will be generated in the first term however. Squaring the second term and exhibiting only terms that are of the W-fusion type we obtain

$$-\frac{1}{M_Z^2}\Bigg[\, M_Z^4 A_1\cdot A_1^* + 4c_w^4 M_Z^2|F_1|^2 + M_Z^2|F_2/D_H|^2 \\ -2c_w^2 F_1 k_2^\nu\left(M_Z^2 A_1^\nu + M_Z^2 F_2\frac{M_Z^2}{D_H}k_1^\nu + M_Z^2 R_1^\nu\right)^* + c.c. \\ +F_2\frac{M_Z^2}{D_H}k_1^\nu\left(M_Z^2 A_1^\nu + M_Z^2 R_1^\nu\right)^* + c.c. + ...\Bigg]\,. \quad (2.85)$$

On the second line of this expression (2.85), k_2^ν will generate the same *off-shell* terms, O_{12}, in a manner identical to that of the previous subsection. These terms will cancel in the same way they did in (2.79) and (2.82). Thus the second line of (2.85) is equal to

$$-2c_w^2 F_1 M_Z^2\left[(\frac{1}{2}-2c_w^2)F_1^* + A^* F_2^*\right]\,. \quad (2.86)$$

Next we consider the third line of (2.85). This corresponds to the interference of the contracted Higgs graph $k_1^\mu T_H^{\mu\nu}$ with whatever has remained. The index ν is now carried by the four momentum k_1 instead of k_2. This will not affect the *off-shell* terms generated by the W fusion graphs which will be again O_{12},

$$M_Z^2 k_1^\nu A_1^\nu = M_Z^2 h_1 + M_Z^2 c_w^2 O_{12}F_2\,, \quad (2.87)$$

with

$$h_1 = \frac{V^\alpha}{W_1}\frac{U^\beta}{W_2}\Bigg[-c_w^2 g_{\alpha\beta}\left(\frac{D_2}{D_1}+\frac{D_1}{D_2}\right) \\ +2c_w^2(k_{1\alpha}k_{2\beta}-k_{2\alpha}k_{1\beta})\left(\frac{1}{D_1}-\frac{1}{D_2}\right) \quad (2.88) \\ +\left([g_{\alpha\beta}M_W^2+(1-4c_w^2)k_{1\alpha}k_{1\beta}\right]\left(\frac{1}{D_1}+\frac{1}{D_2}\right)\Bigg]\,.$$

On the other hand, k_1^ν acting on the remainder of the T_{Wf} graphs R_1^ν now generates *off-shell* terms with the opposite sign from the ones that would be generated from k_2^ν. This can easily be seen by looking at the expression for R_1^ν in (2.76). For $\not{k}_1$ to pinch the propagator $1/(\not{q}_4+\not{k}_2)$ we must use momentum conservation to write $\not{k}_1 = -\not{k}_2 + \not{p}_1 + \not{p}_2$, thus introducing a minus sign and a remainder proportional to $\not{p}_1+\not{p}_2 = \not{k}_1+\not{k}_2$ which can give zero pinch. The final result will assume the form

$$k_1^\nu R_1^\nu = c_w^2 M_Z^2 O_{12}F_2 + \cdots \quad (2.89)$$

Thus we observe that the *off-shell* terms in this case do not cancel between (2.87) and (2.89). The third line of (2.85) is then equal to

$$F_2\frac{M_Z^2}{D_H}\left[M_Z^2 h_1^* + 2\cdot c_w^2 M_Z^2 O_{12}F_2^* + ...\right]\,. \quad (2.90)$$

Since the *off-shell* terms that have survived in this interference of the Higgs graph do not contain any fermion propagator, they must be included in the expression for the squared W-fusion graphs and will therefore be a part of our final result. (Actually their numerical significance in the final result is negligible.) Similar results are also obtained for the third term of (2.84) with the replacement $k_1 \leftrightarrow k_2$.

Finally we collect together all terms that do not contain any fermion propagators, that is, all those that resemble the structure of a squared W-fusion graph, and omit all others. In this manner we are able to define a part of the squared matrix element specific to W-fusion:

$$\overline{|T|}^2 = \overline{|T|}^2_{ww} + \dots\,. \quad (2.91)$$

This squared amplitude will play the rôle of the signal for W-fusion, while all remaining squares and interferences will be identified as background. We stress again that this separation between signal and background is now meaningful since both parts are gauge invariant and well behaved at high energies. The signal squared amplitude for W-fusion is explicitly given by

$$\overline{|T|}^2_{ww} = \frac{1}{4}\left[T^{F\mu\nu}T^{*F}_{\mu\nu} - M_Z^2 A_1\cdot A_1^* \right. \\ -M_Z^2 A_2\cdot A_2^* + (1/4-8c_w^2)|F_1|^2 \\ +|F_2|^2\left(|A|^2 - 2M_Z^2/|D_H|^2 - 4M_W^2 O/|D_H|^2\right) \\ \left.+\Re e(F_1F_2^*A^*) - 2M_Z^2\Re e\left(hF_2^*/D_H^*\right)\right]\,, \quad (2.92)$$

where $h = h_1 + h_2$ and

$$O = (q^2 - M_H^2)(W_1+W_2)(1/D_1+1/D_2)\,. \quad (2.93)$$

We observe that the O term changes sign above and below the resonance as an interference term usually does. Finally, the unpolarized W-fusion cross section can be calculated from

$$d\hat{\sigma}_{ww} = \frac{g^4}{2s}\overline{|T|}^2_{ww}\frac{1}{2}d\Phi_4 \quad (2.94)$$

Since in arriving at the result of (2.92) we have accounted for all possible exchange of terms and cancellations between W-fusion and $T_{Wf}+T_{ff}$ graphs, this expression should now respect unitarity. By direct numerical calculation (see below) we can see that this is indeed the case; (2.94) exhibits good high energy behaviour. In fact the cross section assumes a slow logarithmic growth with increasing scattering energy, exactly as in the production of an *on-shell* Higgs. Furthermore the Higgs resonance is clearly exhibited in the differential distribution $d\sigma/dM_{ZZ}$ where $M_{ZZ} = (k_1+k_2)^2 = q^2$.

Since the kinematics allow q^2 to be equal to M_H^2, in order to carry out the numerical evaluation of (2.94) the propagator of the Higgs boson must be regulated. We adopt here the naive approach of adding an imaginary part, equal to the total decay width of the Higgs, to all the Higgs propagator denominators in (2.92). Specifically, we make the substitution

$$D_H = q^2 - M_H^2 + iM_H\Gamma_H\,. \quad (2.95)$$

The width Γ_H is taken to be the sum of all partial, constant decay widths of the (Standard Model) Higgs boson, each one contributing as the relevant threshold is crossed. With all fermions apart from the top quark taken as massless, this is given by[3]

$$\Gamma_H = \theta(q^2 - 4m_t^2)\ \Gamma_H^{(tt)} + \theta(q^2 - 4M_W^2)\ \Gamma_H^{(WW)} + \theta(q^2 - 4M_Z^2)\ \Gamma_H^{(ZZ)}\ . \tag{2.96}$$

Including a constant width in this manner is to some extent an *ad hoc* assumption, but we have found that it works very well numerically.

For a more consistent approach one has to rely on field theory. In field theory, regulators for resonant amplitudes are naturally provided through resummation of the self-energy diagrams which form a geometric series. The minimal approach, sufficient to regulate the resonance, is to include only the imaginary part of the one-loop self energy in the resummation. This corresponds to replacing the inverse Higgs propagator by

$$D_H = q^2 - M_H^2 \to q^2 - M_H^2 + i\Im m\Pi_{HH}(q^2) \tag{2.97}$$

thus giving rise to a running width

$$\Im m\Pi_{HH}(q^2) = \sqrt{q^2}\ \Gamma_H(q^2)\ . \tag{2.98}$$

Since the bosonic parts of the Higgs self energy are gauge dependent, the pinch technique must be used in both the construction and resummation of the self energies [10]. This results in a gauge independent running width that coincides, at $q^2 = M_H^2$, with the physical decay width of (2.96), term by term, viz.

$$\begin{aligned} \Im m\Pi_{HH}^{(tt)}(M_H^2) &= M_H\Gamma_H^{(tt)}, \\ \Im m\Pi_{HH}^{(WW)}(M_H^2) &= M_H\Gamma_H^{(WW)}, \\ \Im m\Pi_{HH}^{(ZZ)}(M_H^2) &= M_H\Gamma_H^{(ZZ)}\ . \end{aligned} \tag{2.99}$$

The resummation of the Higgs self energy alone distorts the Higgs related Ward identities such as (2.27). This is because now the inverse Higgs propagator contains terms of $\mathcal{O}(\alpha)$. To compensate for this and still maintain the Ward identities, we must also include in our amplitude the one-loop imaginary parts of the relevant Higgs vertices. The full form of the Ward identity of (2.27) is [10]

$$k_1^\mu k_2^\nu \Gamma_{\mu\nu}^{HZZ}(q,-k_1,-k_2) + M_Z^2\Gamma^{H\chi\chi}(q,-k_1,-k_2) = \frac{igM_Z}{2c_w}\left[D_H(q^2) - D_\chi(k_1^2) - D_\chi(k_2^2)\right]\ , \tag{2.100}$$

where χ is the Goldstone boson related to the Z gauge boson. A similar Ward identity holds for the $\Gamma_{\mu\nu}^{HWW}$ vertex. These are Ward identities relating the tree level vertices and propagators of the classical Lagrangian. They hold true before including ghost and gauge fixing terms. They are still valid at one loop for the pinch technique Green's functions. At tree level, setting $D_\chi(k^2) = k^2$ in (2.100), since χ is massless before quantization, one recovers (2.27).

However these Ward identities are in fact irrelevant for the unitarity cancellations that we have considered, i.e. those between the W-fusion graphs and the graphs T_{Wf} or T_{ff}. They *will* become essential when one attempts to separate out the Higgs graph alone from the rest of the W-fusion graphs, and to require for it good high energy behaviour. In this case D_H in (2.100) will cancel the Higgs propagator and thus extract a piece from the Higgs graph that combines with the gauge boson graphs, while the rest of the terms in (2.100), namely $\Gamma^{H\chi\chi}$ and D_χ, will remain in the Higgs graph. This is a cancellation 'internal' to the W-fusion graphs. The extra vertex terms in the Higgs graph will however modify its contribution by $\mathcal{O}(\alpha)$. It is conceivable that these terms, if not correctly included, may lead again to violation of unitarity. However since they are $\mathcal{O}(\alpha)$ this would come about only at extremely high energies.

In our approach we have neglected all such terms of $\mathcal{O}(\alpha)$ in the numerator of the Higgs graph. However, in order to obtain an estimate of the difference between our naive treatment and the correct treatment on the resonance, we have calculated the differential cross section using both a constant width and the pinch technique running width for the Higgs. We have only found negligible numerical differences of $\mathcal{O}(10^{-3} - 10^{-4})$. These do not affect any of the plots we present below. In general we believe that the numerical significance of these terms is very small.

The squared amplitude of (2.92) is calculated with `FeynCalc` and a `Fortran` output in terms of scalar products between momenta and fermion currents is obtained. The phase space integration is done by Monte Carlo methods using `VEGAS`. We decompose the phase space according to the structure of the Higgs graph, i.e. to the product of a three body phase space times a two body decay of the Higgs:

$$d\Phi_4(q_1,q_2;q_3,q_4,k_1,k_2) = (2\pi)^3 d\Phi_3(q_1,q_2;q_3,q_4,q)\ dq^2 \times d\Phi_2(q;k_1,k_2)\ . \tag{2.101}$$

3 The process $pp \to ZZ + 2$ jets $+ X$

In this section we investigate the quantitative impact of our results by studying the realistic case of heavy Higgs production at the LHC. In particular, we focus on the ZZ final state (the 'gold-plated' decay channel for a heavy Standard Model Higgs, see for example [1]) We require, in addition, two forward 'tag' jets [11], so that the leading-order subprocess is $qq \to qqZZ$. We will compare the cross sections obtained using the full scattering electroweak amplitude for this process [3] with those obtained using the pinch-approximated W-fusion amplitude, as defined and calculated in the previous section.

[3] Recall that we are interested only in heavy Higgs bosons, decaying to Z^0Z^0 final states, whose total width is dominated by the $t\bar{t}$, W^+W^- and Z^0Z^0 contributions.

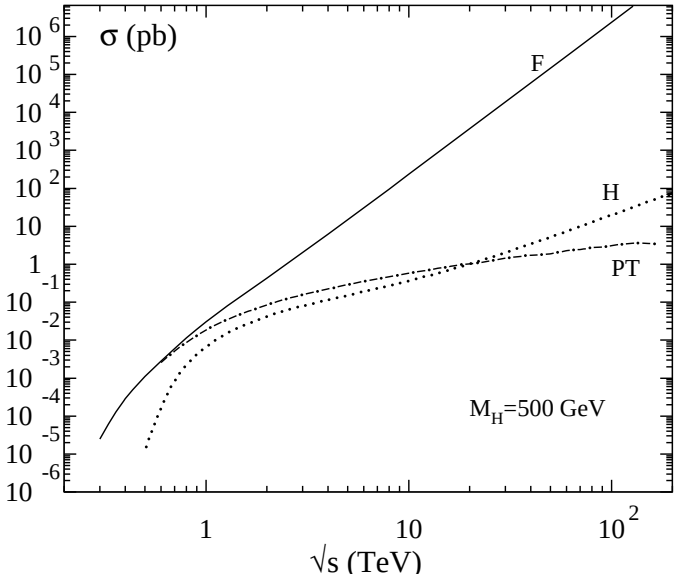

Fig. 7. Total subprocess cross section for W-fusion. The solid line represents the six W-fusion graphs in the Feynman gauge. The dotted line is the Higgs graph alone. The dash-dotted line is the pinch technique result

The full cross section is obtained by summing over all possible parton subprocesses folded with the appropriate parton distributions:

$$\sigma(pp \to ZZ + 2j + X) = \sum \int dx_1 dx_2 f_{q_1/p}(x_1, Q^2) \times f_{q_2/p}(x_2, Q^2) \hat{\sigma}(q_1 q_2 \to q_1' q_2' ZZ) \; . \tag{3.1}$$

For the parton distributions we use the default MRST set [12], with scale choice $Q = M_H$. As our primary aim is to compare cross sections calculated using different scattering amplitudes, we fix the parton and parameter choices throughout the study, and impose the same cuts on the final-state particles. Because it is physically indistinguishable, we must include also the resonant Z-fusion contribution. The Z-fusion amplitude can be obtained straightforwardly from the relevant 3 Feynman graphs, since they form a gauge invariant subset. In some of the subprocesses one of the two resonant mechanisms appears as Higgs-strahlung S graphs, which are suppressed relative to the fusion graphs by an additional factor of $\hat{s}$. In such cases we retain only the energetically dominant, fusion one. For example, in $\bar{u}u \to \bar{d}dZZ$ the Higgs-strahlung S_{ZZ} graphs are suppressed. When they are both relevant, as in $du \to udZZ$ for example, we will neglect the interference between them. This is because the momenta of the final state quarks are crossed in the Z-fusion graphs relative to the W-fusion quark momenta. Since each amplitude peaks in the forward region there is a negligibly small region of overlap in phase space. For the same reason, when calculating amplitudes with identical fermions in the final state we will not consider the crossed diagrams, including only the direct one without the symmetry factor 1/2.

We begin by showing, in Fig. 7, the total subprocess cross section as a function of the subprocess centre-of-mass energy $\sqrt{s}$, calculated three different ways. For purposes of illustration we take $M_H = 500$ GeV. The solid line (F) correponds to the six W-fusion graphs calculated in the Feynman gauge. As discussed in the Introduction, this exhibits the unitarity-violating behaviour $\sigma \sim s^2$ at high energy. Isolating the Higgs resonance graph alone (dotted line H) again leads to unitarity-violating behaviour, but now $\sigma \sim s$.[4] Finally, applying the pinch technique as described in the previous section yields acceptable high-energy behaviour of the form $\sigma \sim \ell n(s)$ (dash-dotted line PT).

The 'bad' high-energy behaviour of the W-fusion graphs completely swamps the Higgs resonance behaviour. This is illustrated in Fig. 8, which shows the ZZ invariant mass distribution at two values of the subprocess energy $\sqrt{s}$, again for $M_H = 500$ GeV. For the W-fusion graphs contribution, we see the resonance at 500 GeV disappear under the background as $\sqrt{s}$ increases. At high $\sqrt{s}$ the cross section is spread approximately uniformly over the range $(0, \sqrt{s})$. In contrast, applying the pinch technique gives invariant mass distributions in which the resonance is clearly visible at both values of $\sqrt{s}$ considered. Of course the extent to which the Higgs resonance is visible over the underlying non-resonant diagram contributions depends on Γ_H. Figure 9 shows the same ZZ (pinch-technique) mass distribution as in Fig. 8, for $M_H =$ 500 GeV and $\sqrt{s} = 4$ TeV, together with the corresponding distributions for $M_H = 750$ GeV and 1000 GeV. Notice that, as expected, the resonant peak broadens as M_H increases, becoming barely visible over the non-resonant contributions at $M_H = 1000$ GeV.

Our final two figures show distributions for the *full* ($\sqrt{s} = 14$ TeV) proton-proton cross section, i.e. with parton distributions folded in as in (3.1). In these figures we compare the pinch-technique (approximate) result with the full all-diagrams calculation of [3]. Figure 10 shows the ZZ invariant mass distributions for $M_H = 500$ GeV and $M_H = 740$ GeV. We see that the resonance region is indeed very well approximated by the pinch-technique result. The high-mass tail is also in good agreement with the full result. Only the low M_{ZZ} region below $\mathcal{O}(400$ GeV) shows any significant difference. Here the large number of non-W-fusion graphs in the full calculation leads to an excess over the pinch-technique result. We note, however, that this low-mass region would in all likelihood be removed by experimental cuts in a realistic analysis.

It is relevant to ask whether other features of the final state are well approximated by the pinch-technique method. As an illustration, we consider the transverse momentum distribution of the forward jets accompanying the Z boson pair. Since it may be possible to detect these jets in the LHC experiments, it is important that the pinch-technique result gives an accurate description of their production properties. Figure 11 shows the predictions for the inclusive jet p_T distribution in the full calculation and the pinch-technique approximation, for $M_H = 500$ and

[4] Notice also the threshold behaviour of this contribution at $\sqrt{s} \simeq M_H$.

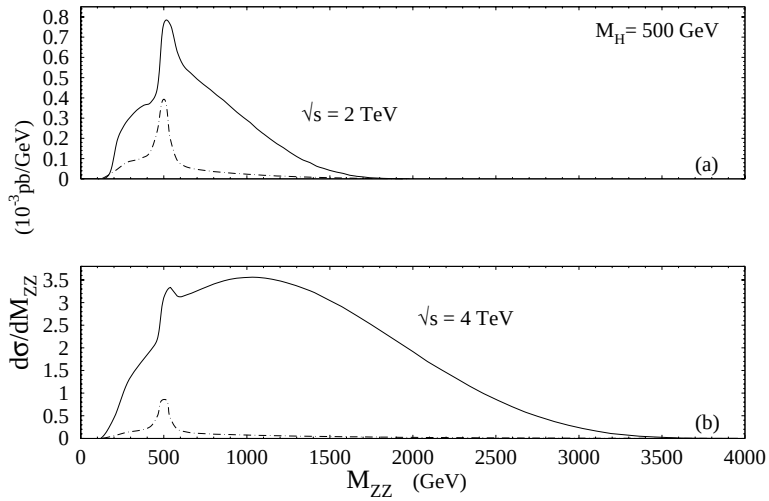

Fig. 8. Invariant mass distribution of the Z boson pair. The solid line is the pinch-technique result while the dotted line is the result of the 6 W-fusion graphs

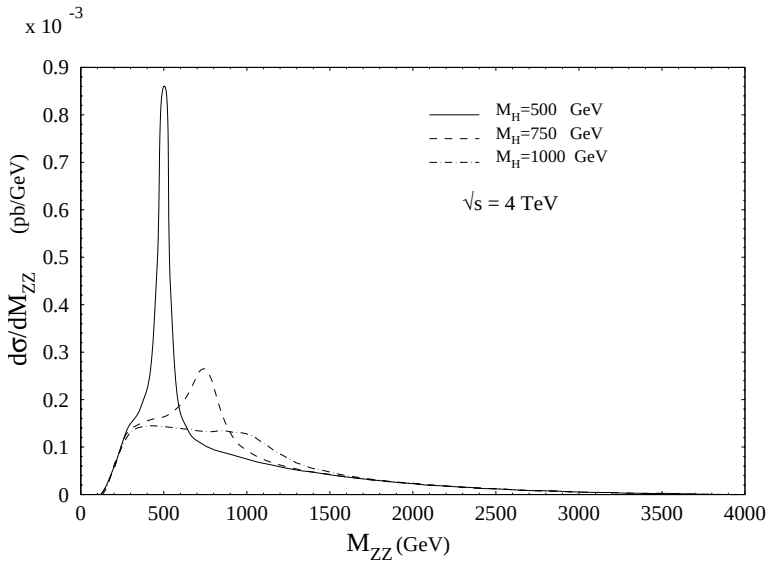

Fig. 9. Invariant mass distribution for the Z boson pair of the pinch-technique result, for different values of the Higgs mass and for subprocess scattering energy $\sqrt{s} = 4$ TeV

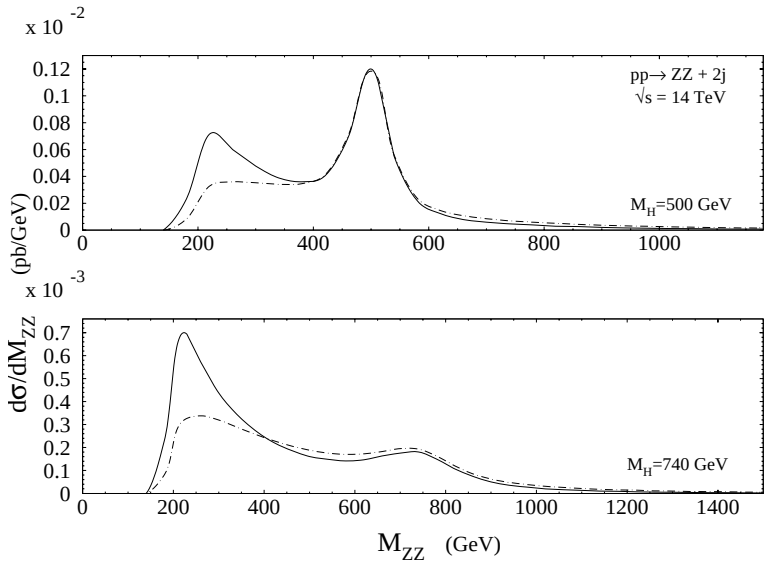

Fig. 10. Invariant mass distribution of the Z boson pair for $pp \to ZZ + 2$ jets $+ X$ at the LHC. The solid line represents the full calculation in which all electroweak graphs are included. The dashed-dotted line is the pinch-technique approximation in which only the resonant W-fusion and Z-fusion graphs are retained

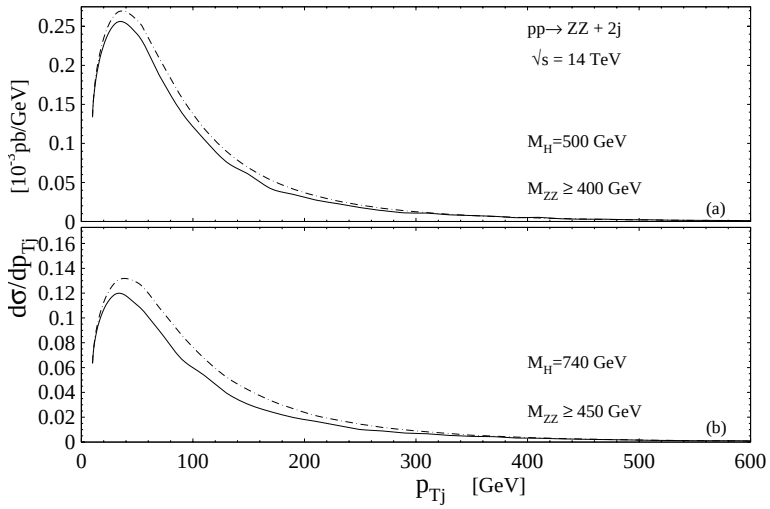

Fig. 11. Distributions of the jet transverse momentum for $pp \to ZZ + 2$ jets $+ X$ at the LHC. The solid line represents the full calculation in which all electroweak graphs are included. The dashed-dotted line is our approximation in which only the resonant W-fusion and Z-fusion graphs are retained

740 GeV. A lower M_{ZZ} cut is imposed (see above). The distributions are indeed very similar, particularly in shape. (The small pinch-technique excess can be traced back to the slightly higher M_{ZZ} distribution in Fig. 10.) The rapidity distributions of the jets (not shown) are also very similar. This gives us confidence that all important kinematic features of the $ZZ + 2$ jets production process are well reproduced by the pinch-technique method.

4 Conclusions

In this paper we have used the pinch-technique to define and calculate a W-fusion subamplitude of the full amplitude for the electroweak process $qq \to qqZZ$. The pinch-technique amplitude is based on the W-fusion subset of diagrams, and includes the Higgs resonance contribution, i.e. $WW \to H \to ZZ$. More importantly, the pinch-technique amplitude squared is *gauge invariant* and the corresponding cross section exhibits *good high energy behaviour*. In addition, our numerical studies show that the pinch-technique gives an excellent approximation to the full calculation for such quantities as the ZZ invariant mass distribution, particularly in the region of the resonance, and the rapidity and transverse momentum distributions of the jets accompanying the ZZ pair. Not surprisingly, the expression for the pinch-technique is much more compact than that for the full amplitude, with a corresponding computation time per event which is between one and two orders of magnitude faster.

In summary, we have demonstrated, in an non-trivial example, that a *meaningful* and *well defined* separation between *signal* and *background* can be achieved even when they contribute *coherently* to the same final state. In the particular case of interest the *signal* turns out to be dominant while its numerical computation compared to the full cross section has been expedited enormously. We believe, therefore, that the pinch-technique amplitude could be a useful simulation and analysis tool for Higgs production via W-fusion at the LHC.

Acknowledgements. We would like to thank Joannis Papavassiliou for useful discussions and Nigel Glover for providing us with his `Fortran` code of the full calculation. K.P. would also like to thank Matthias Heyssler for help with the drawing of Feynman graphs and Marco Stratmann for technical support and help with `PAW`. This work was supported in part by the EU Programme "Human Capital and Mobility", Network "Phenomenological Studies of Electroweak and Strong Interactions at Future Colliders", contract CHRX-CT93-0319 (DG 12 COMA). The work of K.P. is also supported by a *Marie Curie* TMR grant FMBI-CT96-1033.

References

1. R.K. Ellis, W.J. Stirling, B.R. Webber, QCD and Collider Physics, Cambridge University Press (1996)
2. R. Kleiss, W.J. Stirling, Phys. Lett. B **182**, 75 (1986)
3. U. Baur, E.W.N. Glover, Nucl. Phys. B **347**, 12 (1990); Phys. Rev. D **44**, 99 (1991)
4. J. Papavassiliou, E. de Rafael, N.J. Watson Nucl. Phys. B **503**, 79 (1997)
5. J. Papavassiliou, A. Pilaftsis, Phys. Rev. D **53**, 2128 (1996)
6. G. t' Hooft, Nucl. Phys. B **33**, 173 (1971)
7. J.M. Cornwall, J. Papavassiliou, Phys. Rev. D **40**, 3474 (1989)
8. J.M. Cornwall, D.N. Levin, G. Tiktopoulos, Phys. Rev. D **10**, 1145 (1974); ibid **E11**, 972 (1975); C.E. Vayonakis, Lett. Nuovo Cim. **17**, 383 (1976)
9. J.L. Gervais, A. Neveu, Nucl. Phys. B **46**, 381 (1972); Z. Bern, D.C. Dunbar, Nucl. Phys. B **379**, 562 (1992); Y.J. Feng, C.S. Lam, Phys. Rev. D **53**, 2115 (1996); `hep-ph/9608219`
10. J. Papavassiliou, A. Pilaftsis, Phys. Rev. D **58**, 053002 (1998); Phys. Rev. Lett. **80**, 2785 (1998)
11. R.N. Cahn, S.D. Ellis, R. Kleiss, W.J. Stirling, Phys. Rev. D **35**, 1626 (1986)
12. A.D. Martin, R.G. Roberts, W.J. Stirling, R.S. Thorne, Eur. Phys. J. C **4**, 463 (1998)